UNIVERSITY OF BATH

University of Bath

Image Processing for Quantification of Machining Induced Changes in Subsurface Microstructure

Alborz Shokrani[1*], Vimal Dhokia[1], Joseph M Flynn[1] and Stephen T Newman[1]

[1]Department of Mechanical Engineering
University of Bath
Bath, BA2 7AY, United Kingdom

ABSTRACT

Subsurface microstructure and subsurface microhardness are two important aspects of surface integrity in machining operations to assess the quality of a product. Traditionally, subsurface microstructure is examined using visual metallographic techniques. However, in some cases, visual inspections fail to provide an explanation for changes in the material properties. This paper presents research with three samples of Ti-6Al-4V titanium alloy are machined using dry, wet and cryogenic cooling environments. The subsurface microhardness of the samples is then measured and Scanning Electron Microscope (SEM) micrographs of the subsurface microstructure are produced. A new method is proposed to quantify the SEM micrographs. The proposed method is based on image processing techniques and aims to provide a measurable parameter for the concentration of various phases of material at each given distance below the machined surface. Visual comparison of the results from the proposed method with the subsurface microhardness of the material, indicates that it has a potential to provide a better understanding of the machining induced changes in the subsurface microstructure of workpiece material.

1. INTRODUCTION

Machining is the most common method of generating products by removing the excess material from a block of material with turning, milling and drilling being the most known machining operations. Machinability is a material characteristic which indicates the ease of removing material from a workpiece. It includes tool life, surface integrity, cutting forces and power consumption [1]. Surface integrity is one of the parameters, assessed in order to specify the quality of a final product which can affect the service life of a component. It includes a range of geometrical and material characteristics of a machined part ranging from surface roughness and surface topography to material microstructure and residual stresses.

During machining operations of metallic parts, the heat generated at the cutting zone together with cutting forces can affect the material microstructure of the workpiece. This can be due to mechanical forces resulting in movements of particles and crystals below the machined surface or local heat treatment of the surface or a combination of both. Furthermore, chemical interaction between particles within the workpiece material and with machining environment and cutting tool material can change the characteristics of the workpiece material [2]. These changes can affect the material properties and hardness of the workpiece on and below the machined surface.

In order to identify the effect of machining on the microstructure of a workpiece material, two methods are commonly used by researchers. (i) Microhardness analysis of the workpiece material below the machined surface is used to investigate the variation in microhardness below the machined surface with substrate material. (ii) The other method is to analyse the microstructure of a material on a cross section sample vertical to machining path. In this method, a cross section sample of the workpiece material is prepared, polished and etched for material analysis. An optical metallurgical microscope or scanning electron microscope (SEM) is then used to visually investigate the changes in the microstructure of the material below the machined surface.

El-Wardany et al. [3, 4] studied the effects of various machining parameters on microstructure and microhardness of AISI D2 steel in turning operation. The authors used micrographical method to analyse the microstructure of

---

material below the machined surface. The researchers found that machining heat has resulted in deformation of carbide particles within the workpiece material whilst a thin (2μm) heat affected zone was formed on the machined surface [3]. Examination of the micrographs also indicated that microstructural deformation has taken place up to 15μm beneath the machined surface [3]. Analysis of the subsurface microhardness of the machined samples indicated that the alteration in subsurface material microhardness do not occur beyond 55μm below the machined surface. Furthermore, they noticed that existence of hard carbide particles affects the reading for microhardness resulting in an increased uncertainty of the results [4].

Devillez et al. [5] investigated the effect of dry and wet machining environments on the subsurface microstructure and microhardness of Inconel 718 in turning operation. Visual inspection of micrographs of the material structure indicated incoherent grain size with little plastic deformation of the grain boundaries adjacent to the machined surface. Analysis of the subsurface microhardness revealed a gradient where the microhardness was highest (525HV for dry and 510HV for wet) adjacent to the machined surface and was reduced gradually to the material substrate hardness (430-440HV) at 250μm below the machined surface.

In machining Ti-6Al-4V titanium alloy, Che-Haron and Jawaid [6] noted that machining has resulted in an increased microhardness immediately below the machined surface. The authors associated this higher microhardness to strain-hardening properties of titanium as a result of machining. Furthermore, they reported that the microhardness was less below the machined surface which was associated with over-aging of the material due to the machining temperatures. Micrographs of the subsurface material structure indicated plastic deformation of the grain structures as shown in figure 1.
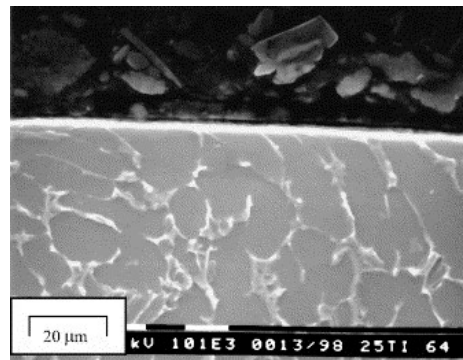

Figure 1: Plastic deformation of microstructural grains in machining Ti-6Al-4V [6]

In another study, Ezugwu et al. reported that no significant changes in the material structure of machined Ti-6Al-4V alloy were detected as a result of machining operation. However, a reduction in material microhardness was detected below the machined surface. The authors [7] attributed this change to the tempering of the material close to the machined surface due to the heat generated during cutting operation.

These studies indicated that visual inspection of micrographs of material microstructure is insufficient to explain changes in the subsurface microhardness of the material. This study intends to propose a new method based on image processing techniques to quantify the micrographical results of subsurface microstructure of machined materials. Ti-6Al-4V titanium alloy is selected for this study and the proposed method was tested for three samples machined under three different machining environments of dry, wet and cryogenic cooling. Subsurface microhardness of the samples is also measured to compare with the results from the proposed method.

2. SAMPLE PREPARATION FOR EXPERIMENTS

The selected workpiece material for this study is Ti-6Al-4V titanium alloy which is one of the most used materials in aerospace industries due to its high specific material strength. Three blocks of titanium with 100mmx50mmx50mm were prepared for machining experiment. The machining operation consisted of end milling with a 12mm diameter solid carbide cutting tool under three machining environments of dry, wet and cryogenic. The machining was performed using 30m/min cutting speed, 0.03mm/tooth feed rate and 1mm depth of cut.

In order to identify the effects of cryogenic machining on the microstructure of Ti-6Al-4V alloy and measure the depth of microstructural damage due to machining, a cross-sectional image of the microstructure of the machined

samples are required. A slice of material perpendicular to the machining path has been cut from each machined block using a band saw at low speed as shown in figure 2a. The slices have an approximate thickness of 20 mm and have been cut from the center of each block to prevent the effects of tool instability at the start and end of each machining path as shown in figure 2.

The machined area of the samples was cut using an abrasive cutter and the samples were mounted in resin in a way that the cross-section of the machined zone is facing upward (figure 2b). In order to prepare the samples for microstructural analysis, each sample was ground and polished to 50nm. The samples were ground using P400 grit paper until plane and then polished at three stages using 9μm and 3μm liquid diamond and finally 0.05μm silica.
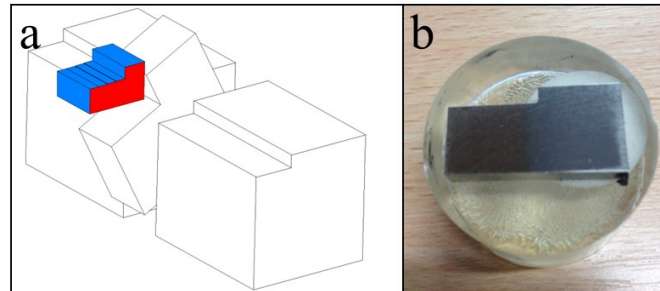

Figure 2: Cutting position of the sample used for analysis (a) and sample used for analysis (b)

The effect of machining on the subsurface microstructure of the workpieces was investigated using two different techniques. (i) The subsurface microhardness of the workpieces was measured using a Leco M400 microhardness tester with 100gr load applied for 15 seconds. Due to the apparatus restrictions, the microhardness was measured at 10μm intervals below the machined surface up to 3mm and measurements closer than 10μm to the machined surface was not applicable. (ii) Furthermore, composition back scattered electron imaging (BEI) scanning electron microscope (SEM) was used to generate micrographs of the subsurface microstructure of the samples.

3. RESULTS OF SUBSURFACE MICROHARDNESS AND MICROSTRUCTURE ANALYSIS

As shown in figure 3, analysis of microhardness of the samples beneath the machining surface indicated that the hardness of the material has been affected up to 100μm below the surface irrespective of machining environment. However, the most noticeable change has taken place in the first 20μm below the machined surface. The microhardness was observed to be lowest for cryogenic machining being followed by dry and wet conditions respectively. The microhardness was gradually increased beneath the machined surface and reached a peak at 40-50μm below the machined surface. After 50μm, the microhardness has declined and reached the material substrate hardness at 100μm.
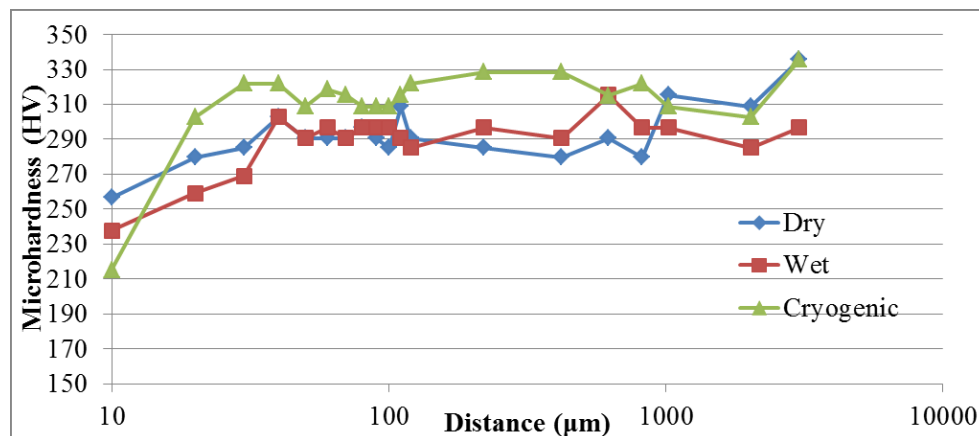

Figure 3: Subsurface microhardness graph for samples machined at different machining environments

SEM micrographs of the cross section of the machined samples are shown in figure 4. Visual inspection of SEM micrographs revealed that no significant change has taken place in the microstructure of material below the machined surface. As illustrated in figure 4, due to the variations in crystal formation within samples, no noticeable changes can be seen in the microstructure of the material as a result of changes in the machining environment. Furthermore, visual investigation of the images does not reveal any change detectable by eye on the material structure below the machined surfaces. Moreover, no correlation between the microhardness and subsurface microstructure is detectable by the human eye.
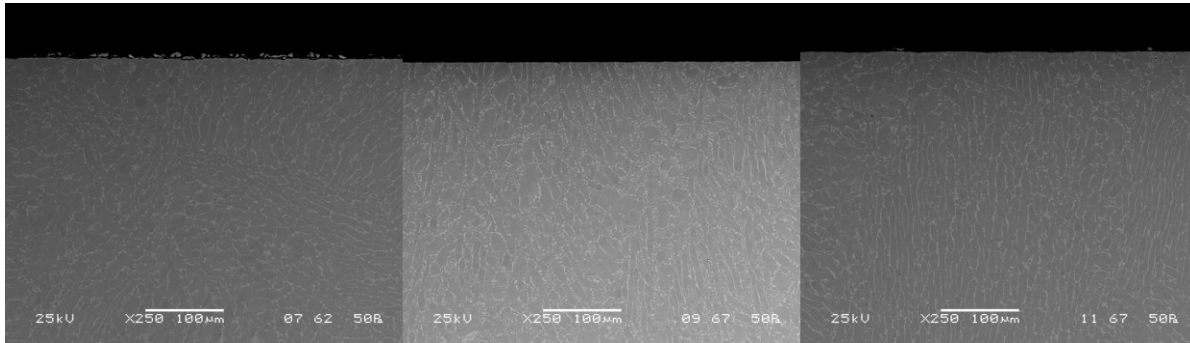

Figure 4: Subsurface microstructure of samples machined under dry, wet and cryogenic environments

4. PROPOSED IMAGE PROCESSING METHOD FOR QUANTIFICATION OF MICROSTRUCTURE SEM GRAPHS

As explained in the results section, visual inspection of the SEM micrographs for cross section of machined samples failed to explain the changes in the subsurface microhardness of the samples. As a result, an image processing method has been implemented using Matlab [8] in order to compare the concentration of β phase beneath the machined surface. As shown in figure 4, the Ti-6Al-4V samples consist of course α plates which are surrounded by a thin layer of β phase titanium. Since the β phase appears brighter than the α phase, a binary image of the cross section can help identifying the changes in the microstructure.

The 250X magnification BEI has been used for image processing. Figure 5 demonstrates the stages conducted for image processing and depicts the image from the sample machined under cryogenic condition as an exemplar. Initially, the images were opened in Matlab as a matrix and cropped in order to remove the areas which do not present the cross section e.g. resin (stage 1). A low pass Gaussian filter has been applied on the images in order to reduce the noise of the image (stage 2). In order to put an emphasis on the β phase in the images, Canny's edge detection filter has been applied with various sigma values as shown in stage 3 in figure 5. The Canny method seeks local maxima of gradient using two thresholds to detect strong and weak edges [8].

The generated image of the edges have then been merged into the image from the second stage (stage 4) to form an image with extra emphasis on the β phase of the material. In SEM imaging, any tilt or slope of the sample results in a change in the contrast and brightness across of an image as shown in figure 5 stage 1. In order to eliminate the adverse effect of various contrast and brightness, contrast limited adaptive histogram equalization technique has been performed on the merged image to uniform the contrast and brightness across the image (stage 5). A binary filter has been applied to the normalized image (stage 6) to represent the image in two colors of black and white. In this image, the β phase is presented in white whilst α is black.
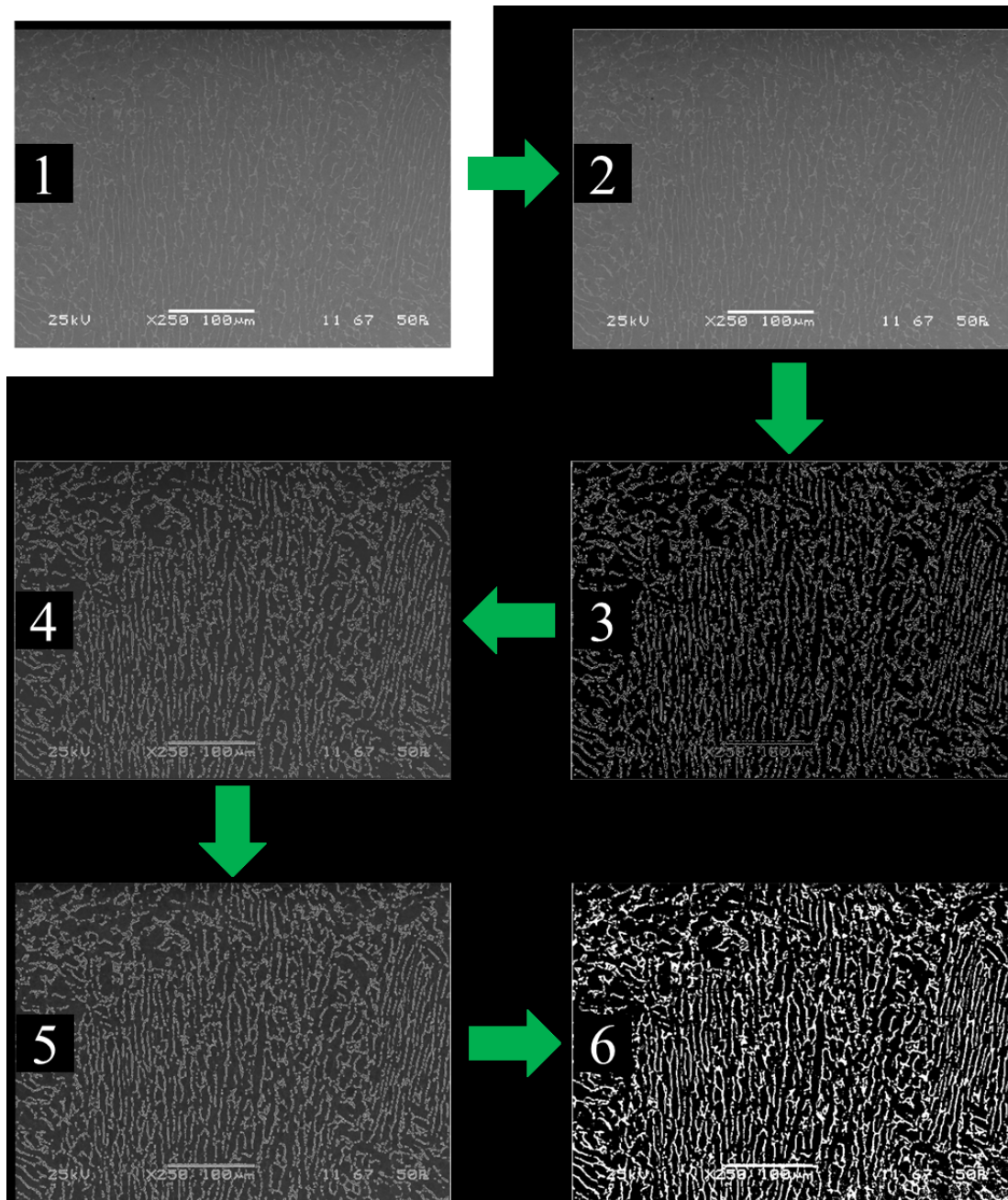
Figure 5: Image processing stages 1 to 6 for preparing the image and improving image quality

As shown in figure 5 (stage 6), the annotations in the image are also in white color which has been transformed into the binary image at the end of the stage 6. Thus, in order to prevent them affecting the analysis, the lower side of the images has been cropped as illustrated in figure 6 (stage 7). In Matlab [8], images are presented in the form of an intensity matrix where each member of the matrix represents the intensity value of its corresponding pixel in the image. Since the image from stage 6 is a binary image, the members of the representing matrix are either 0 or 1. Each member of the matrix represents a 1μm x 1μm square of the material.

In stage 8 (figure 6), the average white pixel concentration (AWPC) for each 1μm beneath the machined surface have been calculated using the intensity matrix. As shown in figure 6 (stage 8), the corresponding data of the AWPC has been plotted which indicated a highly noisy data. Thus, a moving average filter with span of 10 has been applied in order to smooth the data for AWPC (stage 9). Furthermore, a curve has been fitted to the filtered data to represent the

trend of the AWPC beneath the machined surface (stage 10). Visual comparison of the curve generated for AWPC with microhardness below the machined surface implies that a reduction in the AWPC and therefore β phase has resulted in reduced microhardness below the machined surface. Figure 7 illustrates a comparison between the graphs generated for microhardness with the curve fitted for AWPC for the cryogenic sample.
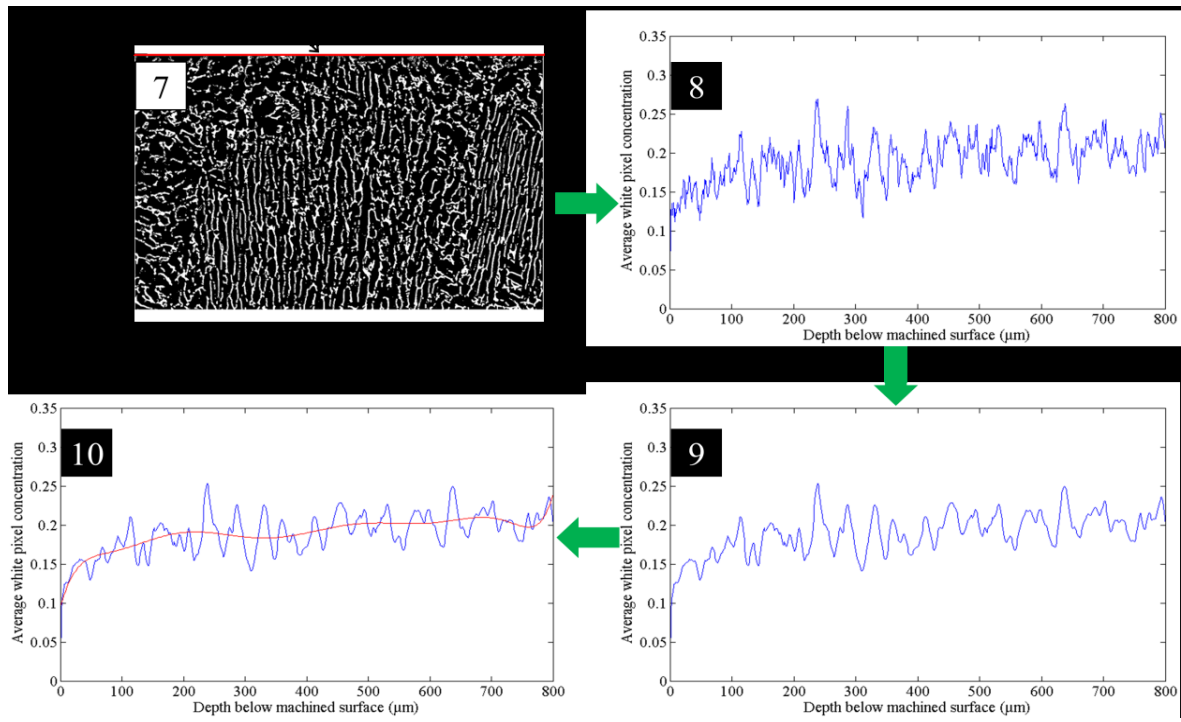

Figure 6: Image processing stages for quantification of the image
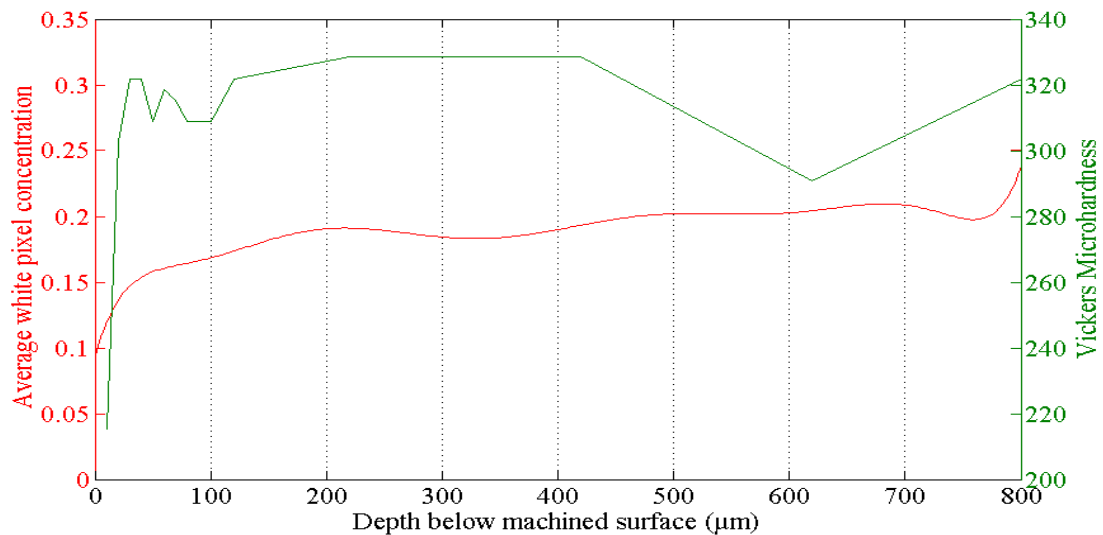

Figure 7: Comparison of subsurface microhardness graph with average white pixel concentration

Studying the graphs generated for AWPC against depth below the machined surface in figure 8, demonstrates that the AWPC and consequently β phase titanium increases as the depth below the machined surface increases. This indicates that cutting operation affects the concentration of β phase titanium irrespective of machining environment. As shown in figure 8, examining the AWPC graphs indicated that the effect of machining on the microstructure of the material is shallower under cryogenic cooling as compared to dry and wet conditions. The depth of machining affected zones for different machining environments is shown with vertical lines in figure 8.
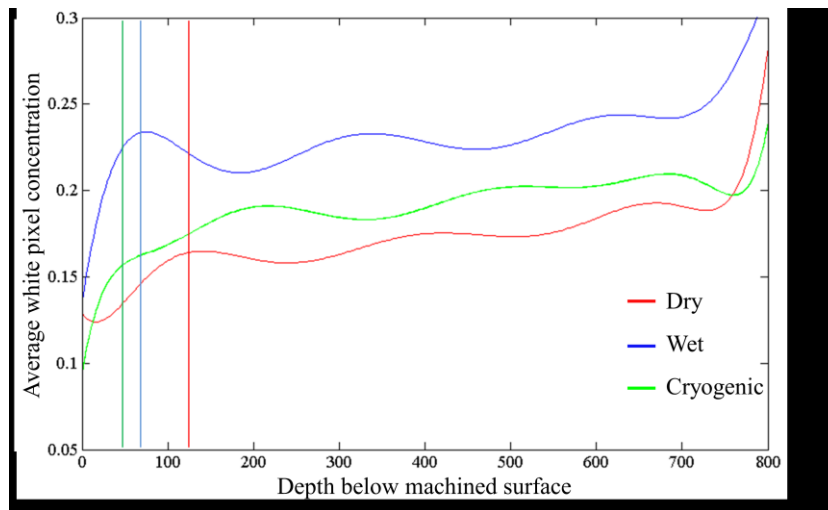

Figure 8: Average white pixel concentration for samples machined under dry, wet and cryogenic conditions

5. DISCUSSION

Analysis of the workpieces showed that the microhardness of the material below the machined surface has been changed up to 100μm below the machined surface as 3. The major part of this change has taken place at the first 20μm below the surface. The material hardness at this depth has been found to be lower than the material substrate which can be due to over-aging of the material at the cutting temperature [6]. The change in microhardness of materials has been observed on all samples irrespective of machining environment.

Due to the low resolution of the microhardness tester equipment, measuring microhardness closer than 10μm to the surface was not applicable as explained in methodology. Thus, no significant difference between the samples of cryogenic and wet machining was observed. Visual examination of micrographs of the subsurface microstructure of the samples indicated that no significant changes in the microstructure took place in cryogenic machining as compared to wet and dry machining. Similar observations were reported by Ezugwu et al [7] in turning of Ti-6Al-4V using high pressure and conventional coolants and by Dandekar et al. [9] in hybrid turning.

Since visual examination of the subsurface microstructure micrographs was not in agreement with the data from microhardness, the image processing technique was implemented to analyse the images quantitatively. This technique has previously been used by researchers [10, 11] to enhance the visual difference between different phases of material microstructure. In addition, Christodoulou [12] used image processing to quantify the grain density and grain size in cast steel. However, to the best of the author's knowledge using average white pixel concentration (AWPC) has not been reported previously.

The quality of this technique is dependent on the quality and size of the image. Sharper images with higher resolutions and wider area can improve the quality of the analysis. In order to cover a larger area of the material and due to the limited field of view of the SEM, the subsurface micrographs were generated at 250x magnification which translates in 1 pixel for each 1μm x 1μm of the material. This prevents the local changes in the material microstructure affecting the results for AWPC. Since the resolution of the SEM is significantly higher that the employed microhardness tester, the comparison between the AWPC graphs and microhardness is considered subjective.

The analysis of the AWPC graphs has indicated that machining has changed the microstructure of the material below the machined surface by reducing the concentration of β phase. This change appears to take place up to almost

100μm beneath the machined surface. This can explain the reduction in microhardness of the material below the machined surface.

6. CONCLUSION

Machining induced material and microstructural changes are one of the important parameters affecting the service life of components. Three samples of Ti-6Al-4V titanium alloy were machined under dry, wet and cryogenic environments to be used for subsurface microstructural analysis and following conclusions can be drawn:

- Visual inspection of the micrographs from subsurface microstructure of machined samples usually fails to explain the changes in the subsurface microhardness due to the limitations of human eye.

- A new method was proposed in this study to quantify the SEM images of subsurface microstructure of machined samples. The method is based on various image processing techniques using Matlab.

- The results from image processing were visually compared with subsurface microhardness graphs for various samples. The proposed method proved to have a potential to facilitate understanding the machining induced changes in material microstructure.

Further studies with more accurate measurement apparatus are required to identify and validate the effectiveness and accuracy of this method. This study was limited to three samples and the results from AWPC were in agreement with subsurface microhardness test for all samples. However, further experiments are required to indicate the sensitivity of the proposed method.

REFERENCES

[1] Y. Kaynak, T. Lu and I. Jawahir "Cryogenic Machining-Induced Surface Integrity: A Review and Comparison with Dry, MQL, and Flood-Cooled Machining", Machining Science and Technology, Vol.18, pp.149-98, 2014.

[2] K. OKUSHIMA and Y. KAKINO "Study on the generating process of machined surface", Bulletin of JSME, Vol.12, pp.141-8, 1969.

[3] T. El-Wardany, H. Kishawy and M. Elbestawi "Surface integrity of die material in high speed hard machining, Part 1: Micrographical analysis", Journal of Manufacturing Science and Engineering, Vol.122, pp.620-31, 2000.

[4] T. El-Wardany, H. Kishawy and M. Elbestawi "Surface integrity of die material in high speed hard machining, Part 2: microhardness variations and residual stresses", Journal of Manufacturing Science and Engineering, Vol.122, pp.632-41, 2000.

[5] A. Devillez, G. Le Coz, S. Dominiak and D. Dudzinski "Dry machining of Inconel 718, workpiece surface integrity", Journal of Materials Processing Technology, Vol.211, pp.1590-8, 2011.

[6] C. H. Che-Haron and A. Jawaid "The effect of machining on surface integrity of titanium alloy Ti–6% Al–4% V", Journal of Materials Processing Technology, Vol.166, pp.188-92, 2005.

[7] E. O. Ezugwu, J. Bonney, R. B. Da Silva and O. Cakir "Surface integrity of finished turned Ti–6Al–4V alloy with PCD tools using conventional and high pressure coolant supplies", International Journal of Machine Tools and Manufacture, Vol.47, pp.884-91, 2007.

[8] MathWorks "MATLAB R2013b." (Natick, MA, USA: The MathWorks Inc.)2013.

[9] C. R. Dandekar, Y. C. Shin and J. Barnes "Machinability improvement of titanium alloy (Ti–6Al–4V) via LAM and hybrid machining", International Journal of Machine Tools and Manufacture, Vol.50, pp.174-82, 2010.

[10] A. Ducato, L. Fratini, M. La Cascia and G. Mazzola "An Automated Visual Inspection System for the Classification of the Phases of Ti-6Al-4V Titanium Alloy." In: Computer Analysis of Images and Patterns: Springer), pp 362-9, 2013.

[11] J. Chrapoński and W. Szkliniarz "Quantitative metallography of two-phase titanium alloys", Materials characterization, Vol.46, pp.149-54, 2001.

[12] P. Christodoulou "Planar Spatial Arrangement of Precipitates in 0.3 C-30Ni 18Cr-0.9 Ti Austenitic Cast Steel Aged at 600° C for 10 h", Journal of Materials Engineering and Performance, Vol.22, pp.1490-504, 2013.